Received: 6 March 2020 | Revised: 28 May 2020 | Accepted: 29 May 2020

DOI: 10.1002/jez.2393

RESEARCH PAPER

JEZ-A ECOLOGICAL AND INTEGRATIVE PHYSIOLOGY WILEY

Is aquaporin-3 involved in water-permeability changes in the killifish during hypoxia and normoxic recovery, in freshwater or seawater?

Ilan M. Ruhr[1] | Chris M. Wood[1,2,3] | Kevin L. Schauer[1] | Yadong Wang[1] | Edward M. Mager[1] | Bruce Stanton[4] | Martin Grosell[1]

[1]Department of Marine Biology and Ecology, Rosenstiel School of Marine and Atmospheric Science, University of Miami, Miami, Florida

[2]Department of Zoology, University of British Columbia, Vancouver, BC, Canada

[3]Department of Biology, McMaster University, Hamilton, ON, Canada

[4]Department of Microbiology and Immunology, Geisel School of Medicine at Dartmouth, Hanover, New Hampshire

Correspondence
Chris M. Wood, Department of Zoology, University of British Columbia, Vancouver, BC V6T 1Z4, Canada.
Email: woodcm@zoology.ubc.ca

Present address
Ilan M. Ruhr, Division of Cardiovascular Sciences, School of Medical Sciences, University of Manchester, Manchester, UK

Edward M. Mager, Department of Biological Sciences, Advanced Environmental Research Institute, University of North Texas, Denton, Texas.

Funding information
University of Miami Maytag Fellowship, Grant/Award Number: To KLS; Maytag Professorship, Grant/Award Number: MG is a Maytag Professor of Ichthyology; Natural Sciences and Engineering Research Council of Canada, Grant/Award Numbers: Discovery Grant to CMW (RGPIN-2017-03843, RGPIN/473-2012); National Institute of Environmental Health Sciences, Grant/Award Number: Grant P42 ES007373 to BS

Abstract

Aquaporins are the predominant water-transporting proteins in vertebrates, but only a handful of studies have investigated aquaporin function in fish, particularly in mediating water permeability during salinity challenges. Even less is known about aquaporin function in hypoxia (low oxygen), which can profoundly affect gill function. Fish deprived of oxygen typically enlarge gill surface area and shrink the water-to-blood diffusion distance, to facilitate oxygen uptake into the bloodstream. However, these alterations to gill morphology can result in unfavorable water and ion fluxes. Thus, there exists an osmorespiratory compromise, whereby fish must try to balance high branchial gas exchange with low ion and water permeability. Furthermore, the gills of seawater and freshwater teleosts have substantially different functions with respect to osmotic and ion fluxes; consequently, hypoxia can have very different effects according to the salinity of the environment. The purpose of this study was to determine what role aquaporins play in water permeability in the hypoxia-tolerant euryhaline common killifish (*Fundulus heteroclitus*), in two important osmoregulatory organs—the gills and intestine. Using immunofluorescence, we localized aquaporin-3 (AQP3) protein to the basolateral and apical membranes of ionocytes and enterocytes, respectively. Although hypoxia increased branchial AQP3 messenger-RNA expression in seawater and freshwater, protein abundance did not correlate. Indeed, hypoxia did not alter AQP3 protein abundance in seawater and reduced it in the cell membranes of freshwater gills. Together, these observations suggest killifish AQP3 contributes to reduced diffusive water flux during hypoxia and normoxic recovery in freshwater and facilitates intestinal permeability in seawater and freshwater.

KEYWORDS

Fundulus heteroclitus, gills, immunofluorescence, intestine, mRNA, osmorespiratory compromise, oxygen deprivation, permeability, protein, western blot

1 | INTRODUCTION

The gills of teleost fish are epithelial tissues in permanent contact with both the external and internal environments. Owing to these interactions, the composition of the external environment has a profound impact on the function of the gills. Indeed, seawater causes persistent water loss across the gills, because it is hyperosmotic to extracellular fluids, whereas freshwater causes diffusive ion loss through the gills, because it is hypoosmotic to extracellular fluids. Seawater teleosts compensate for this water loss by continuous uptake of salts and water by the intestine (solute-coupled water absorption), while the gills manage any excess plasma salt loads (Grosell, 2010; Larsen et al., 2014). In contrast, freshwater teleost gills are the primary sites of salt and water uptake, while the kidneys eliminate excess water (Larsen et al., 2014). Accordingly, the gills of freshwater teleosts are more permeable to water, whereas those of seawater fish stringently regulate salt fluxes (Isaia, 1984). Although seawater and freshwater teleosts maintain remarkably similar plasma osmolalities and ion levels, they do so using substantially different osmoregulatory strategies to preserve homeostasis (Larsen et al., 2014).

Gill function can also be critically affected by shortages in dissolved oxygen (hypoxia), which can perturb osmoregulatory status. Most fish respond to hypoxia by morphological remodeling of the gills, which enlarges their surface area to shorten the diffusion distance of oxygen, but is commonly associated with a detrimental rise in ion and water permeability (Sardella & Brauner, 2007). Thus, there exists an "osmorespiratory compromise" that is defined as a tradeoff between high permeability—to facilitate gas exchange across the gills—and low permeability—to constrain adverse ion and water fluxes (Nilsson, 1986; Sardella & Brauner, 2007).

Ion or water permeability is a dynamic component of branchial gas-exchange capacity that can be independently regulated over time, to maintain osmotic and ion homeostasis (Gonzalez & McDonald, 1992, 1994; Matey et al., 2011; Swift & Lloyd, 1974; Wood et al., 2009, 2007). To some degree, however, many fish suffer from unfavorable ion and/or water fluxes, when there is a need to increase gas-exchange capacities, such as during intense exercise (Onukwufor & Wood, 2018; Postlethwaite & McDonald, 1995; Robertson, Kochhann et al., 2015; Robertson & Wood, 2014; Wood, 1988; Wood & Randall, 1973a, 1973b) or environmental hypoxia (Iftikar, Matey, & Wood, 2010; Matey et al., 2008; Onukwufor & Wood, 2018; Robertson, Val, Almeida-Val, & Wood, 2015; Sollid, De Angelis, Gundersen, & Nilsson, 2003; Thomas, Fievet, & Motais, 1986). Considering that fish allocate up to 10% of their energy budgets to osmoregulation (Bœuf & Payan, 2001) and that hypoxia can impair ATP-dependent transporters (which maintain ion gradients), changes in gill permeability can drastically disrupt ion and water homeostasis.

Surprisingly, most studies on hypoxia-mediated changes in gill permeability have been conducted on freshwater fish, while only a handful exist on seawater fish (Farmer & Beamish, 1969; Hvas, Nilsen, & Oppedal, 2018; Stevens, 1972; Wood et al., 2019). In the context of climate change, as the number of hypoxic zones in the oceans increase (Diaz & Rosenberg, 2008), it is vital that we learn more about the relationship between oxygen deprivation and gill permeability in marine fish. Furthermore, since water flux is one of the main variables when measuring gill permeability, it is also surprising that there are no reports on the roles that aquaporins might play in this process. Given that aquaporins are the main conduits for transcellular water transport in fish (Cerdà & Finn, 2010), obtaining this information would provide a more holistic understanding of branchial responses to variations in ambient salinity or dissolved oxygen.

Recently, we found that seawater killifish have tighter control over branchial transcellular water permeability (unidirectional water-flux rates) and net water permeability (whole-body water-flux rates) than in freshwater, despite the much steeper osmotic gradient in seawater (Table S1; Wood et al., 2019). These observations correlate with lower branchial aquaporin messenger-RNA (mRNA) expression in several seawater-acclimated euryhaline fish that possibly serves to reduce diffusive water loss (Breves et al., 2016; Cutler, Martinez, & Cramb, 2007; Lignot, Cutler, Hazon, & Cramb, 2002; Madsen, Engelund, & Cutler, 2015; Tipsmark, Sørensen, & Madsen, 2010). On the other hand, both hypoxia and normoxic recovery did not affect branchial water permeability in seawater, but considerably lowered it in freshwater (Table S1; Wood et al., 2019). This suggests that the killifish, which is known to be very hypoxia-tolerant, can reduce ion and water permeability, without sacrificing respiratory gas-exchange capacity—like some teleost species (e.g., the Amazonian oscar [Matey et al., 2011; Robertson, Kochhann et al., 2015; Scott et al., 2008; Wood et al., 2009, 2007])—at least in freshwater (Giacomin, Bryant, Val, Schulte, & Wood, 2019; Giacomin, Onukwufor, Schulte, & Wood, 2020). It is possible that hypoxia does not affect branchial water permeability in seawater killifish because it is already near its lower limit (Wood et al., 2019). These data suggest that hypoxia might not affect branchial aquaporin protein abundance in seawater killifish, but suppress it in freshwater.

In the present study, we investigated the role aquaporin-3 (AQP3) might play in the branchial responses to hypoxia and normoxic recovery, both in seawater- and freshwater-acclimated common killifish. Although a plethora of aquaporins have been identified in teleost fish (Cerdà & Finn, 2010; Madsen et al., 2015; Tingaud-Sequeira et al., 2010), we focused on AQP3 because many euryhaline species increase branchial AQP3 transcription when acclimated to freshwater from seawater (Cutler & Cramb, 2002; Deane & Woo, 2006; Lignot et al., 2002; Madsen, Bujak, & Tipsmark, 2014; Moorman, Lerner, Grau, & Seale, 2015; Tipsmark et al., 2010; Tse, Au, & Wong, 2006; Watanabe, Kaneko, & Aida, 2005), including common killifish (Jung, Sato, Shaw, & Stanton, 2012; Whitehead, Galvez, Zhang, Williams, & Oleksiak, 2011; Whitehead, Roach, Zhang, & Galvez, 2011). Furthermore, a verified killifish AQP3 antibody is available (Jung et al., 2012), which enabled us to quantify AQP3 protein abundance and immunofluorescence, along with measuring mRNA expression. In addition, the teleost intestine also expresses AQP3 mRNA (Madsen et al., 2014; Tipsmark et al., 2010), but it

distribution is not well characterized (Lignot et al., 2002). Therefore, we used the killifish antibody to immunolocalize intestinal AQP3 in seawater and freshwater killifish.

We hypothesized that the reduction in diffusive water permeability in freshwater killifish during and following hypoxia observed in our previous study (Wood et al., 2019) would be accompanied by a downregulation in AQP3 protein and mRNA levels in the branchial epithelium. We also hypothesized that as diffusive water permeability is generally higher in freshwater than seawater fish (Evans, 1967; Isaia, 1984; Potts & Fleming, 1970), the relative changes in AQP3 expression during hypoxia would be greater in the former and match our previous physiological data reported in Wood et al. (2019).

2 | MATERIALS AND METHODS

2.1 | Experimental animals

Experiments were performed over a 3-year period (February 2015–April 2017). Adult common killifish of the northern subspecies (*Fundulus heteroclitus macrolepidotus*; 3–7 g, mixed-sex) were collected the preceding October, by Aquatic Research Organisms Ltd. (Hampton, NH), via beach seining of local tidal flats, and held in their facility in 65% seawater at 22°C for several months. After shipment to the University of Miami, they were held at 23–25°C, at a density of 30–50 animals per 50-L tanks, with flow-through dechlorinated freshwater or full-strength seawater, for at least 1 month before experiments. Fish were fed a daily ration of 1.5% body weight, with sinking pellets (50% protein; Purina AquaMax, Shoreview, MN). The ionic composition of the food (Wood, Bucking, & Grosell, 2010) and of Miami freshwater and seawater (Wood & Grosell, 2008) has been reported earlier. Fish were fasted for 24 hr before experiments, which were performed at the acclimation temperature. All procedures followed an approved University of Miami Animal Care Protocol (IACUC no. 13-225).

2.2 | Experimental protocols

All experiments were performed with freshwater and seawater treatments in parallel, as described previously (Wood et al., 2019). Briefly, all fish were subjected to identical pretreatment and transfer protocols to control for behavioral and physiological disturbances. Fish were placed into individual 250-ml Erlenmeyer flasks that were partially submerged in temperature-controlled wet tables (23–25°C), fitted with aeration tubing, and wrapped in black plastic shielding. The aeration tubing bubbled air or nitrogen into the flasks to achieve normoxia (>80% air saturation ≥ 16.5 kPa = 124 Torr) or hypoxia (10% air saturation = 2.1 kPa = 15 Torr; maintained within ±2% saturation during experiments), respectively. For water changes, pre-equilibrated normoxic or hypoxic water was flowed into each flask and target PO_2 was reached within 3 min. Fish were weighed after the completion of the experimental procedures.

To match the handling procedures in the ^3H_2O diffusive water-flux experiments of Wood et al. (2019), fish were first subjected to a 6–8-hr sham-loading period, before they were transferred to the individual flasks, for sampling after 1 hr of normoxia, 3 hr of hypoxia, or 3 hr of normoxic recovery. Three hours of hypoxia was selected, as we have shown it alters branchial water permeability in killifish (Wood et al., 2019). At these times, the fish were quickly euthanized by overdose with neutralized MS-222 (0.8 g/L; pre-equilibrated to the appropriate PO_2) and the eight gill arches were quickly dissected out. For western-blot analyses (N = 10 in both normoxia and hypoxia and N = 8 in normoxic recovery), the gill arches were rinsed and dry-blotted, and then placed in sealed cryovials, flash-frozen in liquid N_2, and stored at −80°C for later analysis. To ensure sufficient protein for western-blot analyses, the gill arches from two fish were subsequently pooled, so effective N-values were 5 in normoxia and hypoxia, and 4 in normoxic recovery. For mRNA expression and immunohistochemistry, the gill arches from separate groups of fish (N = 6 per treatment) were rinsed in Cortland saline and dry-blotted; the left arches were put into RNAlater™ (Ambion, Austin, TX) and stored at 4°C for later real-time quantitative polymerase chain reaction (qPCR) analysis, and the right arches into Z-fix™ (buffered zinc formalin fixative; Anatech Ltd., Battle Creek, MI) and stored at room temperature for later immunohistochemistry. The intestine was similarly rinsed, dry-blotted, and cut into several small sections, some of which were preserved in RNAlater™ and some in Z-fix™.

2.3 | Western-blot analysis

Membrane isolations used a modified procedure described previously (Tresguerres, Katoh, Fenton, Jasinska, & Goss, 2005). Briefly, frozen gill samples were ground to a fine powder, with a liquid N_2-chilled CryoGrinder (OPS Diagnostics, Lebanon, NJ). Approximately, 1 ml of homogenization buffer (250 mM sucrose, 1 mM ethylenediamine tetraacetic acid, 30 mM Tris, and 1x Halt protease inhibitor cocktail [Thermo Fisher Scientific, Rockford, IL], and pH 7.4) was added for every 400 μg of ground tissue, and cells were lysed via sonication on ice, with two 10-s pulses, allowing 30 s to cool between pulses. The cell lysates were cleared via a 10-min, 3,000-g spin, at 4°C, after which the supernatant was retained, and a small aliquot was taken as the whole-cell lysate. Membranes were pelleted from the remaining lysate via a 60-min, 20,800-g spin, at 4°C. The resulting supernatant was retained as the cytoplasmic fraction, and the pellet was resuspended in 1x radioimmunoprecipitation buffer (150 mM NaCl, 50 mM tris, 1% Triton X-100, 0.5% sodium deoxycholate, 0.1% sodium dodecyl sulfate, and pH 7.6). Protein concentrations were determined by Pierce BCA assays (Thermo Fisher Scientific) and stored at −80°C, until further analysis.

Isolated protein samples (20 μg) were separated on 4–15% tris-glycine gels (Bio-Rad Laboratories, Hercules, CA) and transferred to polyvinylidene fluoride membranes. Membranes were blocked in Pierce Protein-Free Blocking Buffer (Thermo Fisher Scientific), for 1 hr, at room temperature, followed by overnight incubation, at 5°C,

in dilute (1:1,000) killifish AQP3 antibody (Jung et al., 2012) or a commercially available rabbit polyclonal Na^+/K^+-ATPase (NKA) antibody (1:1,000, cat. no. SC-28800; Santa Cruz Biotechnology, Dallas, TX). Blots were then probed with horseradish peroxidase-conjugated donkey anti-rabbit secondary antibody (1:25,000, cat. no. SC-2313; Santa Cruz Biotechnology), for 1 hr, at room temperature. Blots were developed in SuperSignal West Femto Maximum Sensitivity Substrate (Thermo Fisher Scientific) and imaged on a C-DiGit scanner (LI-COR Biosciences, Lincoln, NE). AQP3 band intensity was determined via Image Studio Lite (version 5.0.21; LI-COR Biosciences) and normalized to the total protein, via subsequent Coomassie Brilliant Blue (Thermo Fisher Scientific) staining of the blot (also determined using Image Studio Lite).

2.4 | Complementary DNA synthesis and real-time qPCR

Total RNA was extracted from tissue samples, using RNA STAT-60 solution (Tel-Test Inc., Friendswood, TX) and treated with DNase I (Turbo DNA-Free Kit; Thermo Fisher Scientific). RNA concentration and quality were measured with a Spectra-Drop (SpectraMax Plus 384; Molecular Devices) and confirmed for integrity by gel electrophoresis. Complementary DNA (cDNA) was then synthesized, using SuperScript IV First-Strand Synthesis System (Invitrogen, Waltham, MA), and final products were diluted tenfold in sterile water. A mixture of equivalent volumes from random cDNA samples was prepared as a calibrator.

The qPCR primers (Table S2) were designed using sequence information from the National Center for Biotechnology Information. Products were amplified using a Taq PCR Core Kit (QIAGEN, Germantown, MD), cloned using a TOPO-TA Cloning Kit (Thermo Fisher Scientific), and sequenced to validate target specificity. All qPCR experiments were performed in triplicate (6–7 biological replicates) in a Stratagene Mx4000 instrument (Stratagene, San Diego, CA), using Power SYBR Green Master Mix (Thermo Fisher Scientific). Cycling was as follows: 95°C (10 min), 40 cycles at 95°C (30 s), 58°C (30 s), and 72°C (30 s). The specificity of target amplicon was verified by melting-curve analysis and gel electrophoresis. Relative mRNA expression levels were calculated using the PCR Miner Software (Zhao & Fernald, 2005), normalized to EF1α mRNA expression (which was unaltered by experimental treatments), and expressed relative to the treatment/tissue exhibiting the lowest level of expression. Further details are summarized in the Supporting Information Material.

2.5 | Immunohistochemistry

Following fixation in Z-fix™, gill tissues were immersed in 70% ethanol (~1:20 wt/vol), dehydrated in ascending grades of ethanol, washed in butanol and HistoChoice™ clearing reagent (AMRESCO, Solon, OH), and finally immersed four times in Paraplast Plus™ tissue-embedding medium (Leica Biosystems, Richmond, IL), after which tissues were embedded in tissue molds with Paraplast. Tissues were sectioned at 4 μm, using a Leitz model 1512 microtome (Grand Rapids, MI), and mounted onto poly-L-lysine-coated slides. For steps on how slides were prepared for antibody treatment (i.e., paraplast removal, rehydration, revealing antigenic sites, and nonspecific antigenic blocking), see the Supporting Information Material.

The primary antibodies were monoclonal mouse cystic fibrosis transmembrane conductance regulator (CFTR; cat. no. MAB25031; R&D Systems, Minneapolis, MN) and polyclonal rabbit NKA (cat. no. SC-28800; Santa Cruz Biotechnology). The CFTR antibody has been validated in the Gulf toadfish intestine (Ruhr et al., 2014; Ruhr, Schauer, Takei, & Grosell, 2018) and killifish gills (Marshall, Howard, Cozzi, & Lynch, 2002) by western blot analysis and immunohistochemistry. Likewise, the NKA antibody has been validated in the Gulf toadfish intestine (Ruhr et al., 2014, 2018). The killifish AQP3 antibody (kfAQP3; IACUC registration 50-R-0013) was designed and validated in killifish by western-blot analysis (Jung et al., 2012). To double-stain tissues, the antibodies were diluted to 10 μg/ml, in modified blocking phosphate-buffered saline (PBS; PBS with 0.5% skim milk, 1% bovine serum albumin, and 0.05% Tween-20). Slides were incubated overnight with primary antibodies, in a humidified slide box, with gentle agitation, on an oscillating table (5°C). The next morning, they were rinsed twice in PBS containing 0.05% Tween-20 and once in normal PBS.

The application of secondary antibodies was done in the dark. The secondary antibodies were donkey anti-mouse immunoglobulin G (IgG) secondary antibody for CFTR (Alexa Fluor 488, cat. no. AB_2556542; Thermo Fisher Scientific) and donkey anti-rabbit IgG secondary antibody for NKA or AQP3 (Alexa Fluor 568, cat. no. A10042; Thermo Fisher Scientific), diluted to 10 μg/ml (in blocking PBS). Slides were incubated in a humidified slide box for 1 hr, at 37°C, after which they were rinsed as before. ProLong™ Gold Antifade Reagent (Thermo Fisher Scientific) was used to adhere coverslips to each slide. Control slides were treated equally, apart from primary antibody.

Slides were observed with a fluorescent microscope (Olympus, Center Valley, PA), and images were taken with an attached camera (Retiga EXi, Fast 1394; QImaging, Surrey, BC, Canada) and Olympus U-TVO.5XC-2 camera mount, using the same settings. Fiji (Schindelin et al., 2012), iVision, and Gimp softwares were used to quantitatively analyze the images, as relative corrected fluorescence. Further details are summarized in the Supporting Information Material.

2.6 | Statistical analyses

Data were initially checked for normality with a Shapiro–Wilk test and for homogeneity with Bartlett's χ^2 test; when necessary, data were converted using logarithmic or square-root transformations. Data were analyzed for statistical significance by generalized linear models, using Bonferroni corrections for pairwise comparisons, with SPSS 25 (IBM, Armonk, NY). All tests were two-tailed and significance was accepted when $p \leq .05$. All data are reported as means ± standard error of the mean. Statistical support for the findings (i.e., test statistics,

degrees of freedom, and SPSS-adjusted p values) are given in the Supporting Information Material (Tables S3–S6).

3 | RESULTS

3.1 | Abundance of branchial transport proteins in seawater

Enrichment of NKA protein in the gill (which is known to reside primarily in the basolateral membrane of killifish [Karnaky, Kinter, Kinter, & Stirling, 1976]) was approximately fivefold higher in the cell-membrane fraction, relative to whole-cell lysates (normalized values of 5.39 ± 0.86 vs. 1 ± 0.18), suggesting the membrane enrichment was successful. For internal consistency, the whole-cell, cytoplasm, and membrane fractions of gills from normoxic, hypoxic, and recovery treatments within the same salinity (freshwater or seawater) were each run on the same gel (separate gels for each fraction), and data were normalized to the normoxic treatment for that fraction, as shown in Figure 1 (original blots are shown in Figure S1). Gills from different salinities were also run on different gels; thus, the data could only be quantitatively compared among treatments within each fraction, and not between salinities or between fractions. However, there was enough of the whole-cell fraction from the two salinities to also run both on the same gel, which revealed no significant difference in AQP3 protein abundance between salinities (normalized values of 1 ± 0.08 in freshwater vs. 1.93 ± 0.62 in seawater; $p = .13$).

Branchial whole-cell AQP3 protein abundance in seawater was significantly higher after recovery than during either normoxia or hypoxia, but no significant differences were found in the cytoplasmic or membrane fractions (Figure 1a–c). Elevated whole-cell AQP3 protein abundance in recovered fish gills might be due to higher levels of mRNA in hypoxia (Figure 2a). Indeed, by the end of 3 hr hypoxia, branchial AQP3 mRNA expression in seawater had increased to 290% of normoxic levels.

Furthermore, we also quantified AQP3 protein immunofluorescence in the lamellae and interlamellae of the seawater gills, since this type of spatial resolution was not possible with western-blot analyses. This technique demonstrated that hypoxia did not affect total AQP3 protein immunofluorescence (i.e., combined signal intensity in the lamellae and interlamellae; Figure 3a,b). However, the interlamellar regions of normoxic gills had significantly higher AQP3 immunofluorescence than the lamellar regions. This is exemplified by the very different scales of the y-axis (Figure 3a,b).

In addition to using immunohistochemistry to confirm the presence of AQP3 in seawater killifish gills, we also used CFTR and NKA immunofluorescent antibodies to indicate the membrane-specific location of AQP3. CFTR was abundant in the apical and subapical regions of normoxic gills, but less abundant in hypoxic gills (Figures 4b,c and 4e,f). In general, CFTR was expressed in cells where NKA expression was also prominent, likely ionocytes (chloride cells/mitochondria-rich cells; an example of an apical crypt, composed of high CFTR abundance, on an ionocyte is shown in the inset of Figure 4c). However, only some of the NKA-rich cells expressed CFTR. In both normoxic and hypoxic gills, NKA was localized to the basolateral membrane of the interlamellae and, in hypoxic gills, it was also distributed in the outer margins of the lamellae (Figures 4c and 4f).

AQP3 immunofluorescence had a similar pattern of expression as NKA, in seawater killifish. AQP3 was found on the outer borders of the lamellae and more markedly in the interlamellar regions, where it was clearly localized to the basolateral membranes (Figures 4a,b and 4d,e). On the margins of the lamellae, the situation was less clear; while the pattern was similar to that of NKA, it is possible that AQP3 is expressed both apically and basolaterally. Considering that brightfield images showed red-blood cells spanning almost the entire width of the lamellae, we could not determine the position of either membrane. Moreover, it is also possible that branchial AQP3 is predominantly sub-basolateral or vesicle-bound, which provides an explanation for why AQP3 protein abundance is higher in the whole-cell fraction of recovery fish, but not in the corresponding membrane fraction.

3.2 | Abundance of branchial transport proteins in freshwater

In freshwater gills, there was a trend for reduced AQP3 protein abundance during hypoxia and particularly recovery in all three fractions (Figure 1d–f). In the membrane fraction, the reduction in AQP3 protein abundance was close to significance in hypoxia ($p = .065$) and significantly lower in recovery (Figure 1f). As with the seawater gills, lower AQP3 protein abundance in hypoxia and recovery was also accompanied by a paradoxical hypoxia-mediated elevation in AQP3 mRNA; indeed, it amounted to a significant 67% increase in mRNA expression, relative to control normoxic gills (Figure 2b). In addition, hypoxia caused significant reductions in total branchial AQP3 immunofluorescence, a decrease that was also significant in the lamellar regions (Figure 3c,d). Furthermore, the interlamellae of both normoxic and hypoxic gills displayed significantly more AQP3 immunofluorescence than their lamellar counterparts (Figure 3c,d).

Freshwater gills showed little CFTR immunofluorescence (Figures 4h and 4k), whereas NKA was abundant in the basolateral membrane of the interlamellae and distributed in the outer margins of the lamellae, which seemed unaffected by hypoxia (Figures 4i and 4l). AQP3 was also found on the outer borders of the lamellae and plentifully in the interlamellae in both normoxia and hypoxia (Figures 4g,h and 4j,k). Like in seawater, freshwater gills displayed AQP3 immunofluorescence in the basolateral membrane, but we could not determine its cellular location in the lamellae (Figures 4g,h and 4j,k).

3.3 | Effect of salinity on branchial AQP3 protein abundance

Although we did not find differences in branchial AQP3 protein abundance between salinity acclimations, aside from those of normoxic whole-cell fractions (see above), we observed qualitative

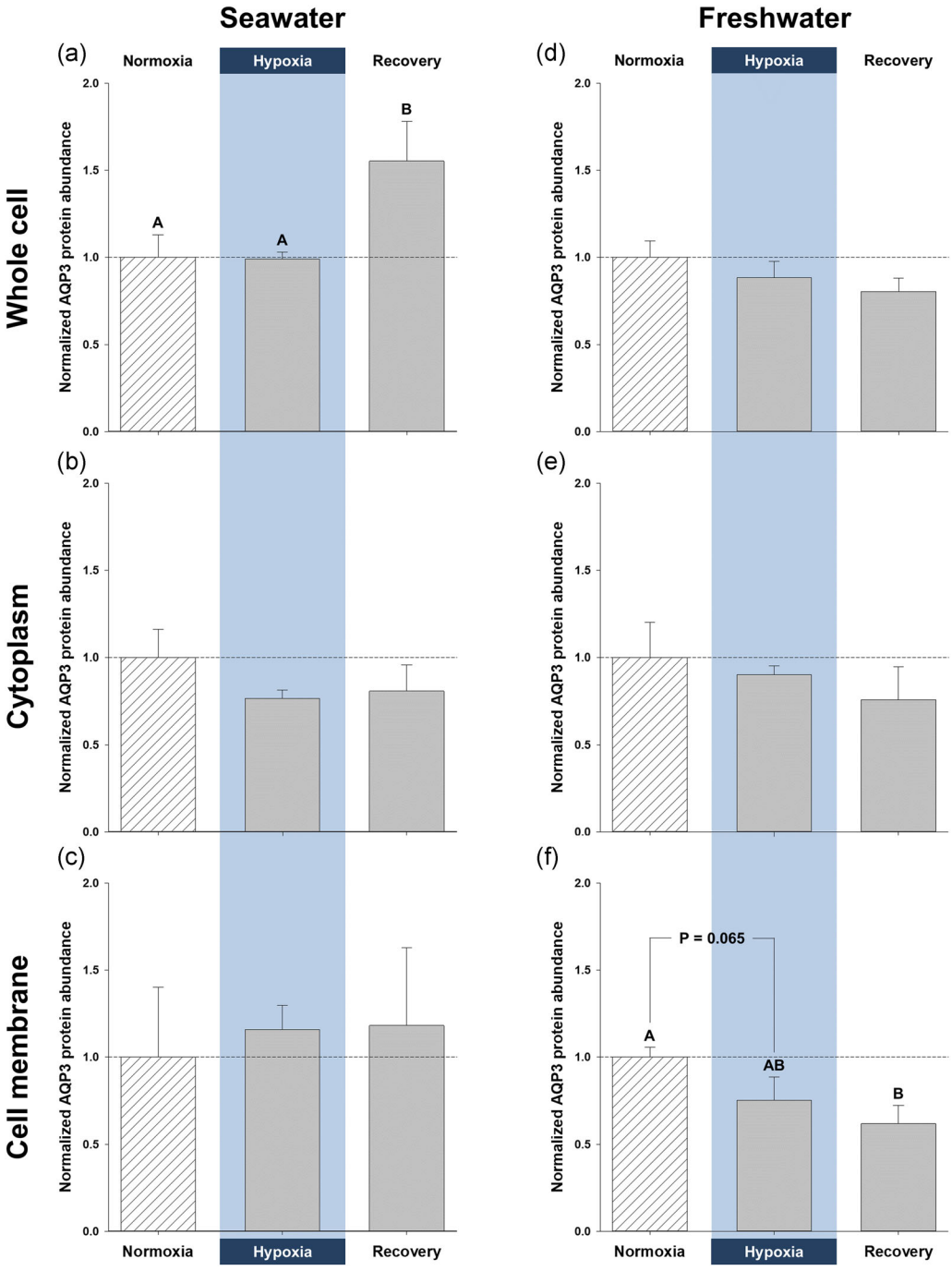

FIGURE 1 Effects of salinity and dissolved oxygen on branchial protein abundance of killifish aquaporin-3 (AQP3). Killifish were acclimated to either seawater or freshwater, and subjected to normoxia (the control), 3 hr hypoxia (10% O_2 saturation), or normoxic recovery, after which the gills were excised. Three fractions were isolated from the gills (whole cell, cytoplasm, and cell membrane) and western blots were run to determine AQP3 protein abundance. (a) Whole-cell, (b) cytoplasmic, and (c) cell-membrane gill fractions of seawater-acclimated fish. (d) Whole-cell, (e) cytoplasmic, and (f) cell-membrane fractions of freshwater-acclimated fish. Data were normalized to normoxic protein levels and are shown as mean ± standard error of the mean (N = 4–5). Significant differences in AQP3 protein abundance between normoxia, hypoxia, and recovery are indicated for oxygen-dependent effects, by dissimilar upper case letters (A and B), when $p \leq .05$. Note that seawater and freshwater samples were run on different gels, so cannot be compared statistically [Color figure can be viewed at wileyonlinelibrary.com]

differences between seawater and freshwater. The gills of seawater-acclimated fish did not alter AQP3 protein levels in hypoxia and responded to normoxic recovery by a general trend for increased AQP3 protein abundance (Figures 1a and 1c), whereas freshwater-acclimated fish subjected to hypoxia and recovery tended to depress AQP3 protein abundance (Figure 1d–f). Quantitatively, freshwater acclimation resulted in significantly higher total AQP3 mRNA expression and total immunofluorescence (both $p \geq .001$), with both

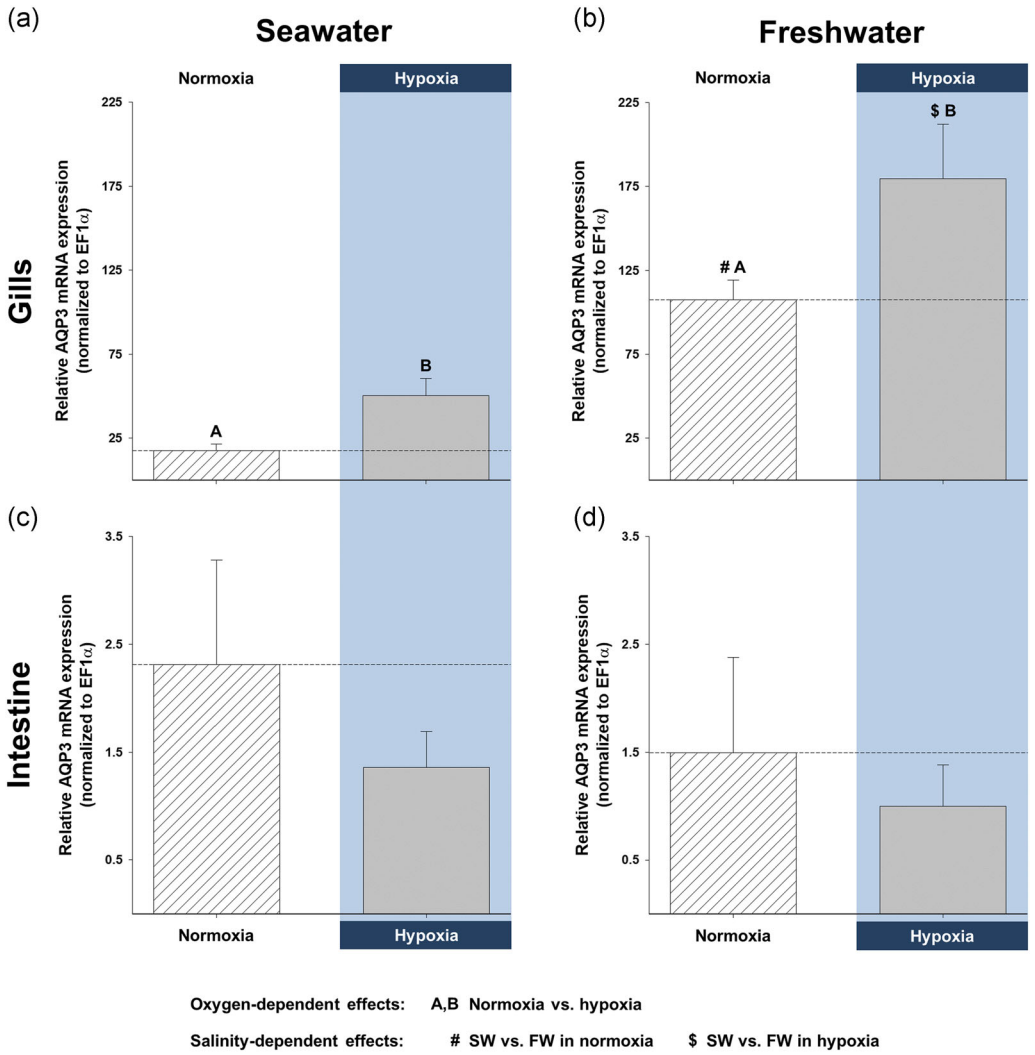

FIGURE 2 Effects of salinity and dissolved oxygen on branchial and intestinal mRNA expression of killifish aquaporin-3 (AQP3). Killifish were acclimated to either seawater or freshwater, and subjected to normoxia (the control) or 3 hr hypoxia (10% O_2 saturation), after which the gills and intestine were excised. Relative AQP3 mRNA expression was determined by real-time quantitative PCR and normalized by calibrating with EF1α. mRNA expression in (a) seawater and (b) freshwater of the gills and in (c) seawater and (d) freshwater of the intestine. Data are shown as mean ± *SEM* (*N* = 6 fish per treatment). Significant differences in AQP3 mRNA expression are indicated for oxygen-dependent effects, by dissimilar upper-case letters (A and B), and for salinity-dependent effects, by pound signs (#) and dollar symbols ($), when $p \leq .05$, as shown in the figure legend (tissue-dependent effects were not analyzed). Although not indicated, freshwater resulted in significantly higher total branchial AQP3 mRNA expression. FW, freshwater; mRNA, messenger RNA; PCR, polymerase chain reaction; *SEM*, standard error of the mean; SW, seawater [Color figure can be viewed at wileyonlinelibrary.com]

normoxic and hypoxic freshwater fish gills exhibiting significantly more AQP3 mRNA than in seawater (Figure 2a,b). Furthermore, freshwater fish lamellae in normoxia and interlamellae in hypoxia displayed significantly greater AQP3 immunofluorescence than their seawater counterparts (Figure 3).

3.4 | Distribution of intestinal transport proteins

Intestinal AQP3 mRNA expression was substantially lower than in the gills and hypoxia did not alter gene expression in either salinity (Figure 5c,d). Nevertheless, the intestine of seawater and freshwater fish displayed AQP3 protein immunofluorescence and we used the immunofluorescent antibodies to localize AQP3 and NKA; material from the hypoxic exposures was not processed. Although we did not quantify the specific intensity of AQP3 immunofluorescence, there appeared to be no differences between the two salinity acclimation groups. AQP3 was abundant in the apical membrane of the enterocytes and in the mucous cells (Figures 5a,b and 5e,f), whereas NKA was plentiful in the basolateral membranes (Figure 5d,h).

4 | DISCUSSION

Numerous studies on fish show that oxygen limitation—either due to environmental hypoxia or strenuous exercise—alters the permeability

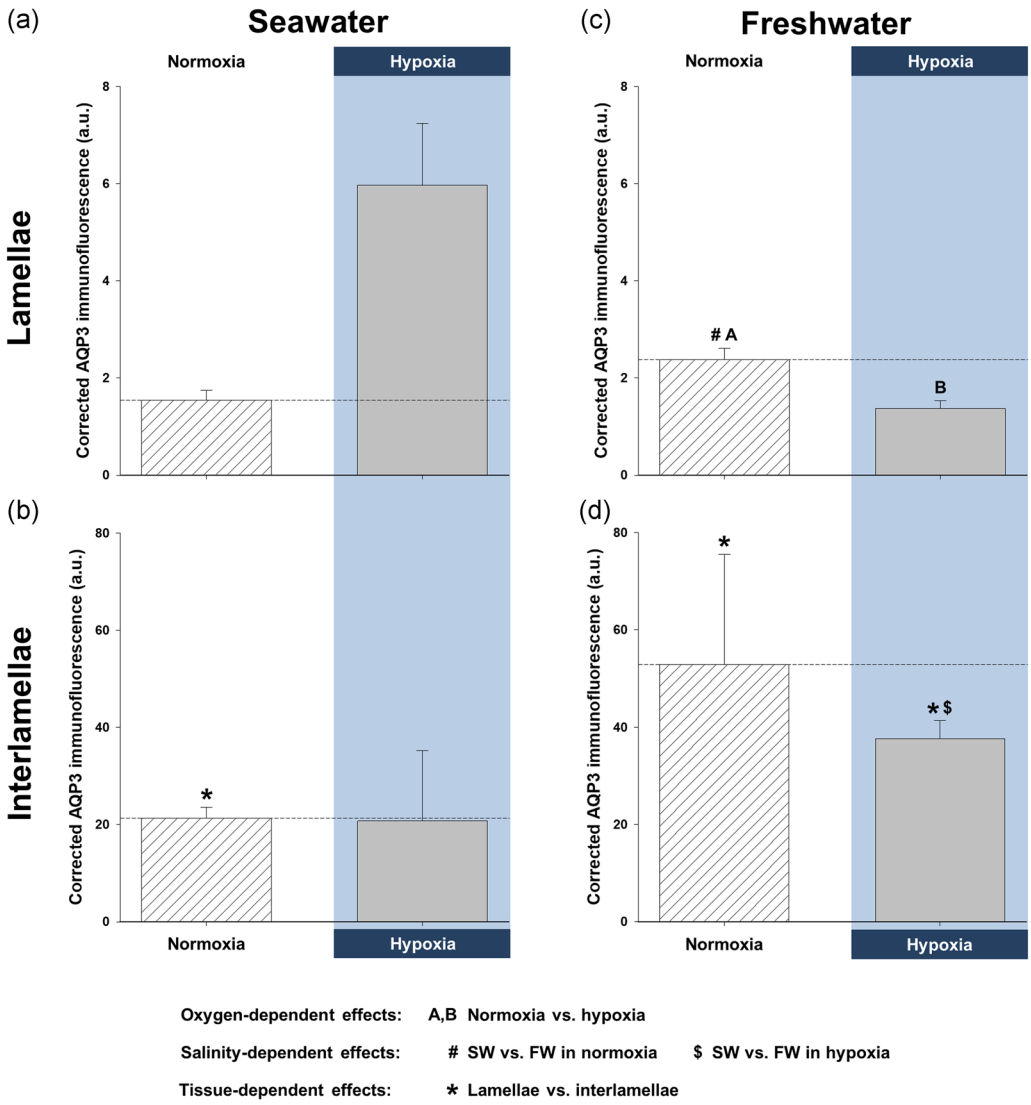

FIGURE 3 Effects of salinity and dissolved oxygen on killifish aquaporin-3 (AQP3) protein immunofluorescence in the lamellae and interlamellae of the gills. Killifish were acclimated to either seawater or freshwater, and subjected to normoxia (the control) or 3 hr hypoxia (10% O_2 saturation), after which the gills were excised. Relative corrected AQP3 immunofluorescence (in arbitrary units [a.u.]) measured in the (a) lamellae and (b) interlamellae of seawater-acclimated fish and in the (c) lamellae and (d) interlamellae of freshwater-acclimated fish. Note the difference in scale between (a) and (c) the lamellae versus (b) and (d) the interlamellae, demonstrating that the majority of AQP3 immunofluorescence is in the interlamellar regions of the gill. Data are shown as mean ± *SEM* ($N = 6$ different fish per treatment). Significant differences in AQP3 immunofluorescence are indicated for oxygen-dependent effects, by dissimilar upper-case letters (A and B), for salinity-dependent effects, by pound signs (#) and dollar symbols ($), and for tissue-dependent effects, by asterisks (*), when $p \leq .05$, as shown in the figure legend. Although not indicated, freshwater resulted in significantly higher total branchial AQP3 immunofluorescence than in seawater, and total AQP3 immunofluorescence was significantly lower in hypoxic versus normoxic freshwater. FW, freshwater; *SEM*, standard error of the mean; SW, seawater [Color figure can be viewed at wileyonlinelibrary.com]

of the gills. Fish enlarge the gill surface area to improve gas exchange across the epithelium, but it is often accompanied by unfavorable ion and water fluxes (see Section 1). This osmorespiratory compromise has been investigated extensively in freshwater, but very few studies have attempted to characterize this response in seawater fish (Farmer & Beamish, 1969; Hvas et al., 2018; Stevens, 1972; Wood et al., 2019) and none have investigated the possible roles aquaporins play.

Here, we show, for the first time, that branchial AQP3 protein abundance and mRNA expression change in a salinity-dependent manner, when common killifish are subjected to hypoxia and normoxic recovery. Our results suggest that there is general agreement with AQP3 protein abundance during hypoxia in seawater and freshwater (Figures 1a,f, and 3) and gill diffusive water fluxes, which is a proxy for transcellular water permeability (Table S1; Wood et al., 2019). Furthermore, our data also suggest that water transport must be strictly regulated during recovery, given that seawater killifish gills increase AQP3 protein abundance, but do not alter transcellular water permeability, while freshwater

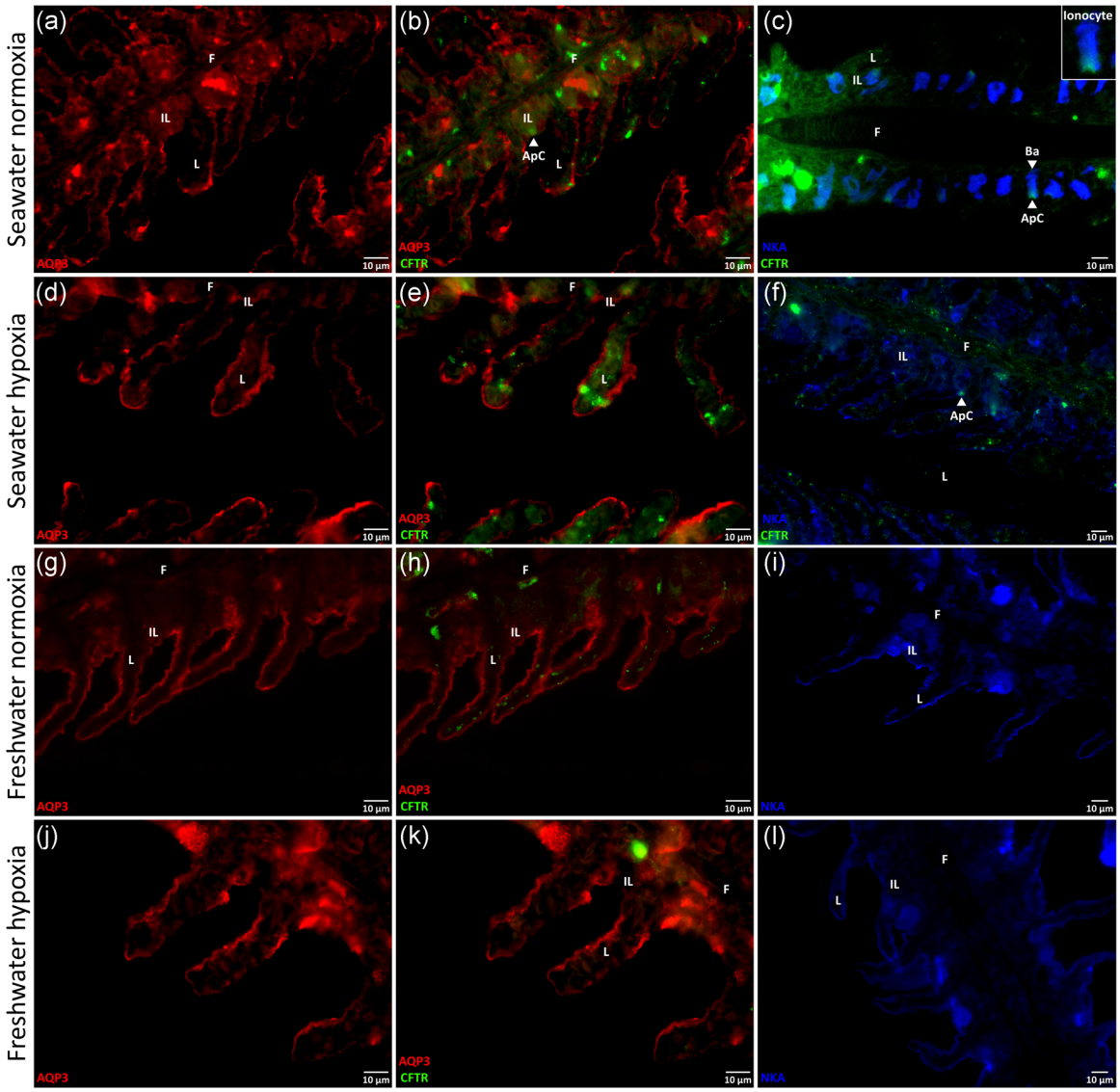

FIGURE 4 Representative immunofluorescent images of aquaporin-3 (AQP3), the cystic fibrosis transmembrane conductance regulator (CFTR), and the Na^+/K^+-ATPase (NKA) in killifish gills. Killifish were acclimated to either seawater or freshwater, and subjected to normoxia (the control) or 3 hr hypoxia (10% O_2 saturation), after which the gills were excised. Immunohistochemistry was used to identify the membrane localization of AQP3 (in red), CFTR (in green), and NKA (in blue), with immunofluorescent antibodies, in seawater (a–c) normoxia or (d–f) hypoxia and in freshwater (g–i) normoxia or (j–l) hypoxia. All immunofluorescent images of AQP3/CFTR are in ×60 and those of NKA are in ×40. AQP3 immunofluorescence generally shared the same distribution as NKA; AQP3 was localized to the basolateral (Ba) membranes (an example is shown on [c]) in both the lamellar (L), and interlamellar (IL) regions of the filaments (F). AQP3 might also occur on the apical membranes at the outer borders of the lamellae. CFTR immunofluorescence was poor in the freshwater gills, but was clearly discernible in the apical membrane of the interlamellae of seawater gills. NKA immunofluorescence was expressed on the basolateral membranes of the cells of the lamella and interlamellae under all treatments and was particularly prominent in the interlamellar regions of the seawater gill under normoxia. Ionocytes (inset on [c]) were apparent in the interlamellar regions of seawater gills under normoxia and hypoxia, and were distinguishable by an apical crypt (ApC; [c] and [f]) expressing CFTR and the basolateral membrane expressing NKA [Color figure can be viewed at wileyonlinelibrary.com]

killifish gills lower both AQP3 protein abundance and transcellular water permeability even further, rather than returning to normoxic levels (Figures 1a,f, and 3; Table S1). Importantly, our results suggest that water-permeability changes in freshwater are associated with modifications in AQP3 protein abundance during and after acute hypoxia.

4.1 | Modulation of AQP3 in normoxic seawater and freshwater

Fluctuations in salinity often alter the distribution and production of branchial ion transporters (Larsen et al., 2014). In killifish gills, for example, freshwater elevates apical Na^+/Cl^--cotransporter (NCC2)

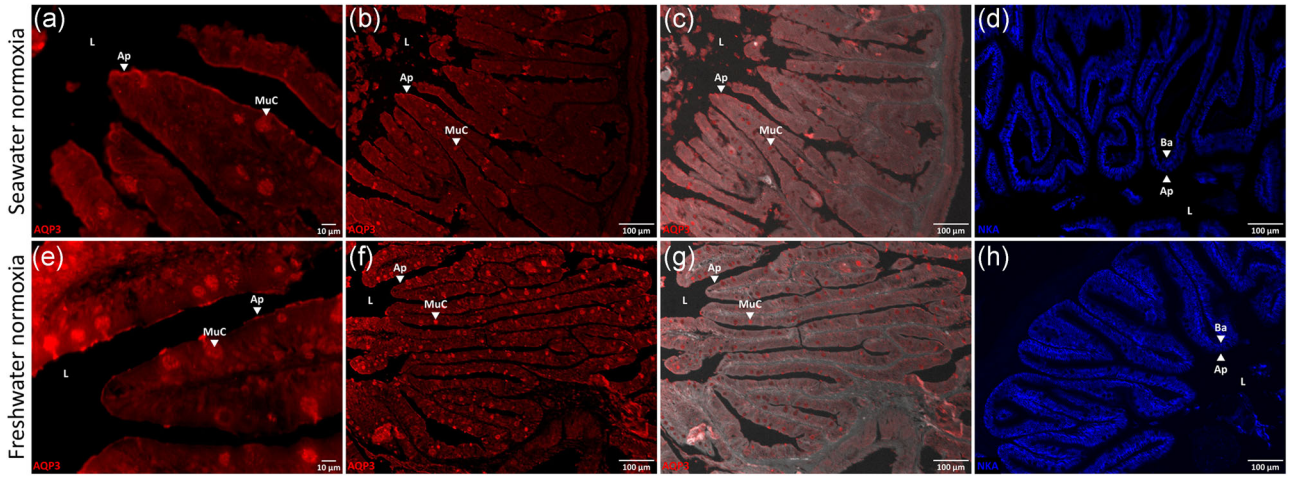

FIGURE 5 Immunofluorescent images of aquaporin-3 (AQP3) and the Na^+/K^+-ATPase (NKA) in the killifish intestine. Killifish were acclimated to either seawater or freshwater, and immunohistochemistry was used to identify the membrane localization of AQP3 (in red) and NKA (in blue), with immunofluorescent antibodies. (a and e) ×60, (b and f) ×10, and (c and g) ×10 brightfield-overlaid images of AQP3 immunofluorescence in the killifish intestine. (d and h) ×10 images of NKA immunofluorescence in the killifish intestine. AQP3 immunofluorescence is localized to the apical (Ap) membrane and mucus cells (MuC) of the enterocytes—facing the intestinal lumen (L)—and is distributed differently than NKA immunofluorescence, which is exclusively basolateral (Ba) [Color figure can be viewed at wileyonlinelibrary.com]

protein and mRNA levels—likely to facilitate ion absorption—and inhibits apical CFTR and basolateral $Na^+/K^+/2Cl^-$-cotransporter (NKCC1) mRNA expression—likely to suppress ion secretion (Breves, Starling, Popovski, Doud, & Tipsmark, 2020). Furthermore, freshwater also increases branchial AQP3 protein abundance and/or gene expression in euryhaline fish (Cutler & Cramb, 2002; Deane & Woo, 2006; Lignot et al., 2002; Madsen et al., 2014; Moorman et al., 2015; Tipsmark et al., 2010; Tse et al., 2006; Watanabe et al., 2005). In combination, such alterations are linked with modified water transport across the gills (Larsen et al., 2014). Likewise, we found higher AQP3 protein immunofluorescence and mRNA expression in the gills of killifish acclimated to freshwater than to seawater (Figures 2 and 3); the greater mRNA levels in freshwater killifish agree with earlier reports on common killifish (Jung et al., 2012; Whitehead, Galvez et al., 2011; Whitehead, Roach et al., 2011). Our observations also parallel the faster control rates of diffusive water exchange (i.e., transcellular water fluxes) in freshwater killifish (Table S1; Wood et al., 2019). However, despite sixfold differences in mRNA expression, there were no differences in seawater versus freshwater whole-cell AQP3 protein abundance, which agree with earlier reports on the killifish (Jung et al., 2012) and the Mozambique tilapia (Watanabe et al., 2005). Conversely, most of the other teleost studies have found freshwater acclimation raises branchial AQP3 protein levels, although these reports show that relative changes in protein abundance are generally smaller than differences in mRNA expression (Deane & Woo, 2006; Lignot et al., 2002; Tse et al., 2006; Watanabe et al., 2005). Such mismatches between mRNA expression and protein abundance are very common (Jung et al., 2012). A variety of factors act to buffer protein concentrations from variations in mRNA levels (Liu, Beyer, & Aebersold, 2016); furthermore, post-translational modification, which can alter aquaporin function, is well-documented (Moeller, Olesen, & Fenton, 2011), and would not be reflected in the western-blot data.

In addition to quantifying changes in protein abundance by western-blot analyses, we also used the kfAQP3 antibody to measure AQP3 protein immunofluorescence in killifish gills. This technique revealed that freshwater acclimation enhanced AQP3 protein immunofluorescence in the gills, particularly under normoxic conditions in the interlamellae (Figure 3). Thus, these results suggest that membrane abundance of AQP3 protein is greater in freshwater, even though gill cells contain roughly equal amounts of AQP3 protein. Such disparities in protein distribution between treatments are not unusual; indeed, branchial CFTR protein abundance is the same in seawater and freshwater killifish, yet more CFTR is found on the cell membranes of seawater gills (Shaw et al., 2008). Taken together, the larger amounts of AQP3 immunofluorescence and mRNA expression in freshwater correlate with the higher diffusive water fluxes in freshwater (Table S1) and suggest a central role for AQP3 in regulating water permeability in killifish gills.

With respect to its branchial distribution in seawater and freshwater, we found AQP3 localized to the basolateral membranes in the interlamellar regions—where ionocytes are most plentiful—and largely to these same membranes in the lamellae—where pavement cells are predominant—though, it is possible that there was also an apical component in the latter (Figure 4). This basolateral distribution in the ionocytes, as well as the occurrence in pavement cells, agrees with previous reports (Breves et al., 2016; Brunelli et al., 2010; Cutler et al., 2007; Lignot et al., 2002; Madsen et al., 2015; Watanabe et al., 2005). However, the cellular distribution of AQP3 in the gills differed in one important aspect from that previously reported in killifish (Jung et al., 2012). Using the identical kfAQP3 antibody in the same species, we detected AQP3 protein immunofluorescence on the

outer borders of the lamellae only (undoubtedly in the pavement cells), whereas the previous study reported AQP3 protein immunofluorescence only in internal pillar cells of the lamellae (Jung et al., 2012). We are aware of no other reports of aquaporins in pillar cells, and the reason for this discrepancy is unknown. Nevertheless, our results agree with the prior report on killifish (Jung et al., 2012) showing the greatest signal in the interlamellar regions (Figures 3b and 3d), where ionocytes are most abundant, with colocalization of AQP3 and NKA in these cells (Figure 4). There is also agreement that AQP3 expression in the lamellae was greater with freshwater acclimation, at least under normoxia (Figures 3a and 3c). However, in contrast to the previous killifish study (Jung et al., 2012), we saw an increased signal in ionocytes in the interlamellar region with freshwater acclimation (Figures 3b and 3d). Again, the prevalence of AQP3 in the lamellae—where surface area is high—in freshwater fits with the greater rate of diffusive water exchange than in seawater, under normoxia (Table S1; Wood et al., 2019).

4.2 | Hypoxia alters branchial AQP3 protein abundance in freshwater but not seawater

In the gills of freshwater killifish, hypoxia lowered AQP3 protein abundance (Figure 1) and immunofluorescence, especially in the lamellae (Figure 3), in support of our hypothesis. These changes in protein abundance mirror the substantial reduction in transcellular water permeability in freshwater (Table S1; Wood et al., 2019), which suggests AQP3 is involved in branchial water transport. On the other hand, hypoxia had no effect on AQP3 protein abundance and immunofluorescence in seawater (Figures 1 and 2), which might explain why transcellular water permeability also does not change (Table S1). In both seawater and freshwater, hypoxia led to greater AQP3 mRNA expression (Figure 2) that was not reflected by corresponding increases in protein abundance or immunofluorescence, perhaps as a result of posttranscriptional modifications (Liu et al., 2016).

Although AQP3 protein abundance and transcellular water permeability are unaffected in hypoxic seawater, paracellular permeability of the gills is considerably reduced, in both seawater and freshwater (Table S1). As stated previously, transcellular water permeability remains unchanged during hypoxia in seawater killifish, possibly because this rate is already at its lower limit in seawater gills. Consequently, by impeding the permeability of the paracellular route, even less water will be lost to the environment. In freshwater, limiting both the transcellular and paracellular permeabilities of the gills (Table S1) will reduce unfavorable water entry. The transcellular permeability reduction would be facilitated by lower AQP3 protein abundance in the cell membrane (Figure 1f). Furthermore, seeing as AQP3 is an aquaglyceroporin that is also permeable to other molecules—glycerol, hydrogen peroxide, urea, and ammonia (Litman, Søgaard, & Zeuthen, 2009; Miller, Dickinson, & Chang, 2010; Verkman, 2012)—reducing AQP3 membrane abundance and, thus, solute efflux might be advantageous. For example, attenuating glycerol loss could be energetically useful, given the switch to triglyceride metabolism during hypoxia (Gracey, Lee, Higashi, & Fan, 2011). As a result, osmoregulatory costs are minimized by both seawater and freshwater killifish in hypoxic water, given that oxygen permeability is likely greatly increased in hypoxia (Giacomin et al., 2019).

We are aware of no other reports on fish investigating the effect hypoxia might have on branchial protein or mRNA levels of aquaporins. Within the 3-hr timeframe of our study, hypoxia would not be expected to cause large changes in absolute AQP3 protein concentration (Liu et al., 2016), and, indeed, this is what we saw (Figure 1). Conversely, owing to the medical implications of perturbed aquaporin function in humans (Soveral, Nielsen, & Casini, 2018), preclinical studies show that oxygen deprivation can suppress aquaporin protein synthesis (e.g., in rodent brain cells [Baronio et al., 2013; Yamamoto et al., 2001]), including AQP3 in the human placenta (Szpilbarg & Damiano, 2017). These reductions might be adaptive responses that limit cellular water flux or programmed cell death. Thus, there seems to be general agreement that vertebrates subjected to oxygen deprivation alter aquaporin protein abundance to reduce osmoregulatory stress.

4.3 | Normoxic recovery alters branchial AQP3 protein abundance differently in seawater and freshwater

Killifish subjected to normoxic recovery exhibited changes in branchial AQP3 protein abundance that were in opposite directions in seawater and freshwater. In seawater, normoxic recovery increased whole-cell AQP3 protein abundance in the gills, but these higher levels of AQP3 were not reflected in the cell membrane (Figure 1). This suggests that AQP3 insertion into the cell membrane does not match its cellular production and/or that gill cells are recycling membrane-bound AQP3 with newly synthesized proteins. Accordingly, the unchanged levels of AQP3 protein in the cell membrane could account for the unaffected transcellular water fluxes observed in seawater gills (Table S1). Paradoxically, normoxic recovery further lowered AQP3 protein abundance in the cell membrane of freshwater gills (Figure 1), which accompanies a continued reduction in transcellular water permeability (Table S1). We might expect both branchial AQP3 membrane protein abundance and transcellular water permeability to be restored to their prehypoxic levels in recovery, but this was not the case. This result suggests that freshwater killifish actively restrict branchial permeability when returned to normoxia, at least during the timeframe of our study. Moreover, the elevation in AQP3 mRNA expression in both hypoxic seawater and freshwater gills could serve as preparatory events for enhanced protein production that is beyond the timeframe of our study (Liu et al., 2016), although this merits further study. In addition, future studies should explore branchial AQP3 mRNA expression and protein immunofluorescence, morphology, and ion fluxes during hypoxia and in normoxic recovery, to further inform us of the roles

aquaporins and other channel proteins play in the physiology of killifish gills.

4.4 | Seawater and freshwater intestines express AQP3 equally

The intestine of seawater teleosts is the organ responsible for water uptake and plays a minor, yet important, role in water influx in freshwater (Grosell, 2010; Marshall & Grosell, 2006). Moreover, the major pathway for fluid absorption in the killifish intestine is transcellular in both seawater and freshwater (Wood & Grosell, 2012). Therefore, we also investigated the distribution of AQP3 in the intestine of killifish acclimated to seawater or freshwater. In contrast to the gills, AQP3 in the intestine was localized to the apical membranes of the enterocytes and to mucous cells (Figure 5). This pattern only partly agrees with observations of the eel gut (Lignot et al., 2002), in which AQP3 expression was reported in only some mucous ("goblet" cells) and macrophages, and not in the enterocytes. Moreover, AQP3 has been found in the gut of other teleost species, but its physiological role has not been extensively studied (Madsen et al., 2015). Regardless, all cells require water and must have the capacity to transport it. Thus, the presence of AQP3 in the killifish intestine is not surprising, but its physiological role should be studied further.

4.5 | Perspective: The potential role of AQP3 in the osmorespiratory compromise during hypoxia

Overall, our data support the conclusion that *F. heteroclitus* is a hypoxia-tolerant species (see Section 1) that can reduce branchial ion and water permeability, while preserving respiratory gas-exchange capacity (Giacomin et al., 2019, 2020; Wood et al., 2019). With respect to regulating water transport, our data suggest that AQP3 plays a role during acute hypoxia and normoxic recovery, at least in freshwater-acclimated killifish. Under normoxic conditions, branchial AQP3 is likely involved in regulating water entry/exit, cell volume, or osmosensing (Cutler et al., 2007; Madsen et al., 2015; Watanabe et al., 2005). We also show that AQP3 is present in the apical membrane of enterocytes in seawater and freshwater, indicating involvement in intestinal permeability. Although AQP1a1 has been implicated in diffusive water exchange in larval zebrafish (Kwong, Kumai, & Perry, 2013) and many other aquaporins occur in fish, we have provided evidence that changes in branchial AQP3 protein abundance correlate with fluctuations in diffusive water fluxes in freshwater killifish. Considering the importance of branchial water permeability, it is surprising how little is known about the regulation and physiological function of aquaporins in the over 30,000 species of teleost fish worldwide.

ACKNOWLEDGMENTS

The work of Chris M. Wood was supported by the Natural Sciences and Engineering Research Council of Canada Discovery Grants RGPIN-2017-03843 and RGPIN/473-2012 and the work of Bruce Stanton was supported by NIEHS Grant P42 ES007373. The work of Kevin L. Schauer was partly supported by a University of Miami Maytag Fellowship. Martin Grosell is a Maytag Professor of Ichthyology. The authors would like to thank Prof. Mike Schmale (University of Miami) for use of his imaging facility and advice on microscopy, Dr. Dawoon Jung (Korea Environment Institute) for advice on immunohistochemistry, and Prof. Patricia Schulte (University of British Columbia) for advice on gene expression.

AUTHOR CONTRIBUTIONS

Conceptualization: C. M. W., I. M. R., K. L. S., and M. G. Methodology: C. M. W., I. M. R., K. L. S., Y. W., and E. M. M. Validation: K. L. S., Y. W., and E. M. M. Formal analysis: I. M. R. and C. M. W. Investigation: I. M. R. and C. M. W. Resources: C. M. W., M. G., and B. S. Data curation: I. M. R., C. M. W., K. L. S., Y. W., and E. M. M. Writing—original draft: I. M. R. and C. M. W.; writing—review and editing: I. M. R., C. M. W., K. L. S., Y. W., E. M. M., B. S., and M. G.; and writing—approval of final version: I. M. R., C. M. W., and M. G. Visualization: I. M. R. Supervision: C. M. W. Project administration: C. M. W. and M. G. Funding acquisition: C. M. W., M. G., and B. S.

ORCID

Ilan M. Ruhr http://orcid.org/0000-0001-9243-7055
Chris M. Wood https://orcid.org/0000-0002-9542-2219
Kevin L. Schauer https://orcid.org/0000-0002-3677-250X
Edward M. Mager https://orcid.org/0000-0001-8992-3095

REFERENCES

Baronio, D., Martinez, D., Fiori, C. Z., Bambini-Junior, V., Forgiarini, L. F., da Rosa, D. P., … Cerski, M. R. (2013). Altered aquaporins in the brains of mice submitted to intermittent hypoxia model of sleep apnea. *Respiration Physiology & Neurobiology*, *185*(2), 217–221. https://doi.org/10.1016/j.resp.2012.10.012

Bœuf, G., & Payan, P. (2001). How should salinity influence fish growth? *Comparative Biochemistry and Physiology Part C: Toxicology & Pharmacology*, *130*(4), 411–423. https://doi.org/10.1016/s1532-0456(01)00268-x

Breves, J. P., Inokuchi, M., Yamaguchi, Y., Seale, A. P., Hunt, B. L., Watanabe, S., … Grau, E. G. (2016). Hormonal regulation of aquaporin 3: Opposing actions of prolactin and cortisol in tilapia gill. *Journal of Endocrinology*, *230*(3), 325–337. https://doi.org/10.1530/JOE-16-0162

Breves, J. P., Starling, J. A., Popovski, C. M., Doud, J. M., & Tipsmark, C. K. (2020). Salinity-dependent expression of ncc2 in opercular epithelium and gill of mummichog (*Fundulus heteroclitus*). *Journal of Comparative Physiology, B: Biochemical, Systems, and Environmental Physiology*, *190*(2), 219–230. https://doi.org/10.1007/s00360-020-01260-x

Brunelli, E., Mauceri, A., Salvatore, F., Giannetto, A., Maisano, M., & Tripepi, S. (2010). Localization of aquaporin 1 and 3 in the gills of the rainbow wrasse, *Coris julis*. *Acta Histochemica*, *112*(3), 251–258. https://doi.org/10.1016/j.acthis.2008.11.030

Cerdà, J., & Finn, R. N. (2010). Piscine aquaporins: An overview of recent advances. *Journal of Experimental Zoology Part A: Ecological Genetics and Physiology*, *313*(10), 623–650. https://doi.org/10.1002/jez.634

Cutler, C. P., & Cramb, G. (2002). Branchial expression of an aquaporin 3 (AQP-3) homologue is downregulated in the European eel *Anguilla anguilla* following seawater acclimation. *Journal of Experimental Biology*, *205*(Pt 17), 2643–2651.

Cutler, C. P., Martinez, A. S., & Cramb, G. (2007). The role of aquaporin 3 in teleost fish. *Comparative Biochemistry and Physiology. Part A, Molecular & Integrative Physiology*, *148*(1), 82–91. https://doi.org/10.1016/j.cbpa.2006.09.022

Deane, E. E., & Woo, N. Y. (2006). Tissue distribution, effects of salinity acclimation, and ontogeny of aquaporin 3 in the marine teleost, silver sea bream (*Sparus sarba*). *Marine Biotechnology*, *8*(6), 663–671. https://doi.org/10.1007/s10126-006-6001-0

Diaz, R. J., & Rosenberg, R. (2008). Spreading dead zones and consequences for marine ecosystems. *Science*, *321*(5891), 926–929. https://doi.org/10.1126/science.1156401

Evans, D. H. (1967). Sodium, chloride, and water balance of the intertidal teleost, *Xiphister atropurpureus*: III. The roles of simple diffusion, exchange diffusion, osmosis, and active transport. *Journal of Experimental Biology*, *47*(Pt 3), 525–534.

Farmer, G. J., & Beamish, F. W. H. (1969). Oxygen consumption of Tilapia nilotica in relation to swimming speed and salinity. *Journal of the Fisheries Research Board of Canada*, *26*(11), 2807–2821. https://doi.org/10.1139/f69-277

Giacomin, M., Bryant, H. J., Val, A. L., Schulte, P. M., & Wood, C. M. (2019). The osmorespiratory compromise: Physiological responses and tolerance to hypoxia are affected by salinity acclimation in the euryhaline Atlantic killifish (*Fundulus heteroclitus*). *Journal of Experimental Biology*, *222*(Pt 19), jeb206599. https://doi.org/10.1242/jeb.206599

Giacomin, M., Onukwufor, J. O., Schulte, P. M., & Wood, C. M. (2020). Ionoregulatory aspects of the hypoxia-induced osmorespiratory compromise in the euryhaline Atlantic killifish (*Fundulus heteroclitus*): The effects of salinity. *Journal of Experimental Biology*. https://doi.org/10.1242/jeb.216309

Gonzalez, R. J., & McDonald, D. G. (1992). The relationship between oxygen consumption and ion loss in a freshwater fish. *Journal of Experimental Biology*, *163*(Pt 1), 317–332.

Gonzalez, R. J., & Mcdonald, D. G. (1994). The relationship between oxygen uptake and ion loss in fish from diverse habitats. *Journal of Experimental Biology*, *190*(Pt 1), 95–108.

Gracey, A. Y., Lee, T. H., Higashi, R. M., & Fan, T. (2011). Hypoxia-induced mobilization of stored triglycerides in the euryoxic goby *Gillichthys mirabilis*. *Journal of Experimental Biology*, *214*(Pt 18), 3005–3012. https://doi.org/10.1242/jeb.059907

Grosell, M. (2010). The role of the gastrointestinal tract in salt and water balance. In M. Grosell, A. P. Farrell & C. J. Brauner (Eds.), *Fish physiology: The multifunctional gut of fish* (30, pp. 135–164). Oxford, UK: Academic Press.

Hvas, M., Nilsen, T. O., & Oppedal, F. (2018). Oxygen uptake and osmotic balance of Atlantic salmon in relation to exercise and salinity acclimation. *Frontiers in Marine Science*, *5*, 368. https://doi.org/10.3389/fmars.2018.00368

Iftikar, F. I., Matey, V., & Wood, C. M. (2010). The ionoregulatory responses to hypoxia in the freshwater rainbow trout, *Oncorhynchus mykiss*. *Physiological and Biochemical Zoology*, *83*(2), 343–355. https://doi.org/10.1086/648566

Isaia, J. (1984). Water and nonelectrolyte permeation. In W. S. Hoar & D. J. Randall (Eds.), *Fish physiology* (10, Part B, pp. 1–38). Amsterdam, The Netherlands: Elsevier.

Jung, D., Sato, J. D., Shaw, J. R., & Stanton, B. A. (2012). Expression of aquaporin 3 in gills of the Atlantic killifish (*Fundulus heteroclitus*): Effects of seawater acclimation. *Comparative Biochemistry and Physiology. Part A, Molecular & Integrative Physiology*, *161*(3), 320–326. https://doi.org/10.1016/j.cbpa.2011.11.014

Karnaky, K. K., Jr., Kinter, L. B., Kinter, W. B., & Stirling, C. E. (1976). Teleost chloride cell. II. Autoradiographic localization of gill Na, K-ATPase in killifish *Fundulus heteroclitus* adapted to low and high salinity environments. *Journal of Cell Biology*, *70*(1), 157–177. https://doi.org/10.1083/jcb.70.1.157

Kwong, R. W., Kumai, Y., & Perry, S. F. (2013). The role of aquaporin and tight junction proteins in the regulation of water movement in larval zebrafish (*Danio rerio*). *PLoS One*, *8*(8), e70764. https://doi.org/10.1371/journal.pone.0070764

Larsen, E. H., Deaton, L. E., Onken, H., O'Donnell, M., Grosell, M., Dantzler, W. H., & Weihrauch, D. (2014). Osmoregulation and excretion. *Comprehensive Physiology*, *4*(2), 405–573. https://doi.org/10.1002/cphy.c130004

Lignot, J. H., Cutler, C. P., Hazon, N., & Cramb, G. (2002). Immunolocalisation of aquaporin 3 in the gill and the gastrointestinal tract of the European eel, *Anguilla anguilla* (L.). *Journal of Experimental Biology*, *205*(Pt 17), 2653–2663.

Litman, T., Søgaard, R., & Zeuthen, T. (2009). Ammonia and urea permeability of mammalian aquaporins. In E. Beitz (Ed.), *Aquaporins* (pp. 327–358). Dordrecht, The Netherlands: Springer.

Liu, Y., Beyer, A., & Aebersold, R. (2016). On the dependency of cellular protein levels on mRNA abundance. *Cell*, *165*(3), 535–550. https://doi.org/10.1016/j.cell.2016.03.014

Madsen, S. S., Bujak, J., & Tipsmark, C. K. (2014). Aquaporin expression in the Japanese medaka (*Oryzias latipes*) in freshwater and seawater: Challenging the paradigm of intestinal water transport? *Journal of Experimental Biology*, *217*(Pt 17), 3108–3121. https://doi.org/10.1242/jeb.105098

Madsen, S. S., Engelund, M. B., & Cutler, C. P. (2015). Water transport and functional dynamics of aquaporins in osmoregulatory organs of fishes. *Biological Bulletin*, *229*(1), 70–92. https://doi.org/10.1086/BBLv229n1p70

Marshall, W. S., & Grosell, M. (2006). Ion transport, osmoregulation, and acid-base balance. *In the Physiology of Fishes*, *3*, 177–230.

Marshall, W. S., Howard, J. A., Cozzi, R. R., & Lynch, E. M. (2002). NaCl and fluid secretion by the intestine of the teleost *Fundulus heteroclitus*: Involvement of CFTR. *Journal of Experimental Biology*, *205*(Pt 6), 745–758.

Matey, V., Iftikar, F. I., De Boeck, G., Scott, G. R., Sloman, K. A., Almeida-Val, V. M. F., … Wood, C. M. (2011). Gill morphology and acute hypoxia: Responses of mitochondria-rich, pavement, and mucous cells in the Amazonian oscar (*Astronotus ocellatus*) and the rainbow trout (*Oncorhynchus mykiss*), two species with very different approaches to the osmo-respiratory compromise. *Canadian Journal of Zoology*, *89*(4), 307–324. https://doi.org/10.1139/Z11-002

Matey, V., Richards, J. G., Wang, Y., Wood, C. M., Rogers, J., Davies, R., … Brauner, C. J. (2008). The effect of hypoxia on gill morphology and ionoregulatory status in the Lake Qinghai scaleless carp, *Gymnocypris przewalskii*. *Journal of Experimental Biology*, *211*(Pt 7), 1063–1074. https://doi.org/10.1242/jeb.010181

Miller, E. W., Dickinson, B. C., & Chang, C. J. (2010). Aquaporin-3 mediates hydrogen peroxide uptake to regulate downstream intracellular signaling. *Proceedings of the National Academy of Sciences of the United States of America*, *107*(36), 15681–15686. https://doi.org/10.1073/pnas.1005776107

Moeller, H. B., Olesen, E. T., & Fenton, R. A. (2011). Regulation of the water channel aquaporin-2 by posttranslational modification. *American Journal of Physiology. Renal Physiology*, *300*(5), F1062–F1073. https://doi.org/10.1152/ajprenal.00721.2010

Moorman, B. P., Lerner, D. T., Grau, E. G., & Seale, A. P. (2015). The effects of acute salinity challenges on osmoregulation in Mozambique tilapia reared in a tidally changing salinity. *Journal of Experimental Biology*, *218*(Pt 5), 731–739. https://doi.org/10.1242/jeb.112664

Nilsson, S. (1986). Control of gill blood flow. In Nilsson & Holmgren (Eds.), *Fish physiology: Recent advances* (pp. 86–101). Dordrecht, The Netherlands: Springer.

Onukwufor, J. O., & Wood, C. M. (2018). The osmorespiratory compromise in rainbow trout (*Oncorhynchus mykiss*): The effects of fish size, hypoxia, temperature and strenuous exercise on gill diffusive water fluxes and sodium net loss rates. *Comparative Biochemistry and*

Physiology. Part A, Molecular & Integrative Physiology, *219–220*, 10–18. https://doi.org/10.1016/j.cbpa.2018.02.002

Postlethwaite, E., & McDonald, D. (1995). Mechanisms of Na^+ and Cl^- regulation in freshwater-adapted rainbow trout (*Oncorhynchus mykiss*) during exercise and stress. *Journal of Experimental Biology*, *198*(Pt 2), 295–304.

Potts, W. T. W., & Fleming, W. R. (1970). The effects of prolactin and divalent ions on the permeability to water of *Fundulus kansae*. *Journal of Experimental Biology*, *53*(Pt 2), 317–327.

Robertson, L. M., Kochhann, D., Bianchini, A., Matey, V., Almeida-Val, V. F., Val, A. L., & Wood, C. M. (2015). Gill paracellular permeability and the osmorespiratory compromise during exercise in the hypoxia-tolerant Amazonian oscar (*Astronotus ocellatus*). *Journal of Comparative Physiology, B: Biochemical, Systems, and Environmental Physiology*, *185*(7), 741–754. https://doi.org/10.1007/s00360-015-0918-4

Robertson, L. M., Val, A. L., Almeida-Val, V. F., & Wood, C. M. (2015). Ionoregulatory aspects of the osmorespiratory compromise during acute environmental hypoxia in 12 tropical and temperate teleosts. *Physiological and Biochemical Zoology*, *88*(4), 357–370. https://doi.org/10.1086/681265

Robertson, L. M., & Wood, C. M. (2014). Measuring gill paracellular permeability with polyethylene glycol-4000 in freely swimming trout: Proof of principle. *Journal of Experimental Biology*, *217*(Pt 9), 1425–1429. https://doi.org/10.1242/jeb.099879

Ruhr, I. M., Bodinier, C., Mager, E. M., Esbaugh, A. J., Williams, C., Takei, Y., & Grosell, M. (2014). Guanylin peptides regulate electrolyte and fluid transport in the Gulf toadfish (*Opsanus beta*) posterior intestine. *American Journal of Physiology. Regulatory, Integrative and Comparative Physiology*, *307*(9), R1167–R1179. https://doi.org/10.1152/ajpregu.00188.2014

Ruhr, I. M., Schauer, K. L., Takei, Y., & Grosell, M. (2018). Renoguanylin stimulates apical CFTR translocation and decreases HCO3-secretion through PKA activity in the Gulf toadfish (*Opsanus beta*). *Journal of Experimental Biology*, *221*(Pt 6), jeb173948. https://doi.org/10.1242/jeb.173948

Sardella, B. A., & Brauner, C. J. (2007). The osmo-respiratory compromise in fish: The effects of physiological state and the environment. In M. N. Fernandes (Ed.), *Fish respiration and environment* (1 ed., pp. 147–165). Boca Raton, FL: CRC Press.

Schindelin, J., Arganda-Carreras, I., Frise, E., Kaynig, V., Longair, M., Pietzsch, T., … Cardona, A. (2012). Fiji: An open-source platform for biological-image analysis. *Nature Methods*, *9*(7), 676–682. https://doi.org/10.1038/nmeth.2019

Scott, G. R., Wood, C. M., Sloman, K. A., Iftikar, F. I., De Boeck, G., Almeida-Val, V. M., & Val, A. L. (2008). Respiratory responses to progressive hypoxia in the Amazonian oscar, *Astronotus ocellatus*. *Respiration Physiology & Neurobiology*, *162*(2), 109–116. https://doi.org/10.1016/j.resp.2008.05.001

Shaw, J. R., Sato, J. D., VanderHeide, J., LaCasse, T., Stanton, C. R., Lankowski, A., … Stanton, B. A. (2008). The role of SGK and CFTR in acute adaptation to seawater in *Fundulus heteroclitus*. *Cellular Physiology and Biochemistry*, *22*(1–4), 69–78. https://doi.org/10.1159/000149784

Sollid, J., De Angelis, P., Gundersen, K., & Nilsson, G. E. (2003). Hypoxia induces adaptive and reversible gross morphological changes in crucian carp gills. *Journal of Experimental Biology*, *206*(Pt 20), 3667–3673. https://doi.org/10.1242/jeb.00594

Soveral, G., Nielsen, S., & Casini, A. (2018). *Aquaporins in health and disease: New molecular targets for drug discovery*. Boca Raton, FL: CRC Press.

Stevens, E. D. (1972). Change in body weight caused by handling and exercise in fish. *Journal of the Fisheries Research Board of Canada*, *29*(2), 202–203. https://doi.org/10.1139/f72-033

Swift, D. J., & Lloyd, R. (1974). Changes in urine flow rate and haematocrit value of rainbow trout, *Salmo gairdneri* (Richardson), exposed to hypoxia. *Journal of Fish Biology*, *6*(4), 379–387.

Szpilbarg, N., & Damiano, A. E. (2017). Expression of aquaporin-3 (AQP3) in placentas from pregnancies complicated by preeclampsia. *Placenta*, *59*, 57–60. https://doi.org/10.1016/j.placenta.2017.09.010

Thomas, S., Fievet, B., & Motais, R. (1986). Effect of deep hypoxia on acid-base balance in trout: Role of ion transfer processes. *American Journal of Physiology. Regulatory, Integrative and Comparative Physiology*, *250*(3 Pt 2), R319–R327. https://doi.org/10.1152/ajpregu.1986.250.3.R319

Tingaud-Sequeira, A., Calusinska, M., Finn, R. N., Chauvigne, F., Lozano, J., & Cerdà, J. (2010). The zebrafish genome encodes the largest vertebrate repertoire of functional aquaporins with dual paralogy and substrate specificities similar to mammals. *BMC Evolutionary Biology*, *10*(1), 38. https://doi.org/10.1186/1471-2148-10-38

Tipsmark, C. K., Sørensen, K. J., & Madsen, S. S. (2010). Aquaporin expression dynamics in osmoregulatory tissues of Atlantic salmon during smoltification and seawater acclimation. *Journal of Experimental Biology*, *213*(Pt 3), 368–379. https://doi.org/10.1242/jeb.034785

Tresguerres, M., Katoh, F., Fenton, H., Jasinska, E., & Goss, G. G. (2005). Regulation of branchial V-H^+-ATPase, Na^+/K^+-ATPase and NHE2 in response to acid and base infusions in the Pacific spiny dogfish (*Squalus acanthias*). *Journal of Experimental Biology*, *208*(Pt 2), 345–354. https://doi.org/10.1242/jeb.01382

Tse, W. K. F., Au, D. W. T., & Wong, C. K. C. (2006). Characterization of ion channel and transporter mRNA expressions in isolated gill chloride and pavement cells of seawater-acclimating eels. *Biochemical and Biophysical Research Communications*, *346*(4), 1181–1190. https://doi.org/10.1016/j.bbrc.2006.06.028

Verkman, A. S. (2012). Aquaporins in clinical medicine. *Annual Review of Medicine*, *63*, 303–316. https://doi.org/10.1146/annurev-med-043010-193843

Watanabe, S., Kaneko, T., & Aida, K. (2005). Aquaporin-3 expressed in the basolateral membrane of gill chloride cells in Mozambique tilapia, *Oreochromis mossambicus*, adapted to freshwater and seawater. *Journal of Experimental Biology*, *208*(Pt 14), 2673–2682. https://doi.org/10.1242/jeb.01684

Whitehead, A., Galvez, F., Zhang, S., Williams, L. M., & Oleksiak, M. F. (2011). Functional genomics of physiological plasticity and local adaptation in killifish. *Journal of Heredity*, *102*(5), 499–511. https://doi.org/10.1093/jhered/esq077

Whitehead, A., Roach, J. L., Zhang, S., & Galvez, F. (2011). Genomic mechanisms of evolved physiological plasticity in killifish distributed along an environmental salinity gradient. *Proceedings of the National Academy of Sciences of the United States of America*, *108*(15), 6193–6198. https://doi.org/10.1073/pnas.1017542108

Wood, C. M. (1988). Acid-base and ionic exchanges at gills and kidney after exhaustive exercise in the rainbow trout. *Journal of Experimental Biology*, *136*(Pt 1), 461–481.

Wood, C. M., Bucking, C., & Grosell, M. (2010). Acid-base responses to feeding and intestinal Cl^- uptake in freshwater- and seawater-acclimated killifish, *Fundulus heteroclitus*, an agastric euryhaline teleost. *Journal of Experimental Biology*, *213*(Pt 15), 2681–2692. https://doi.org/10.1242/jeb.039164

Wood, C. M., & Grosell, M. (2008). A critical analysis of transepithelial potential in intact killifish (*Fundulus heteroclitus*) subjected to acute and chronic changes in salinity. *Journal of Comparative Physiology, B: Biochemical, Systems, and Environmental Physiology*, *178*(6), 713–727. https://doi.org/10.1007/s00360-008-0260-1

Wood, C. M., & Grosell, M. (2012). Independence of net water flux from paracellular permeability in the intestine of *Fundulus heteroclitus*, a euryhaline teleost. *Journal of Experimental Biology*, *215*(Pt 3), 508–517. https://doi.org/10.1242/jeb.060004

Wood, C. M., Iftikar, F. I., Scott, G. R., De Boeck, G., Sloman, K. A., Matey, V., … Val, A. L. (2009). Regulation of gill transcellular permeability and renal function during acute hypoxia in the Amazonian oscar (*Astronotus ocellatus*): New angles to the osmorespiratory compromise. *Journal of*

Experimental Biology, *212*(Pt 12), 1949–1964. https://doi.org/10.1242/jeb.028464

Wood, C. M., Kajimura, M., Sloman, K. A., Scott, G. R., Walsh, P. J., Almeida-Val, V. M., & Val, A. L. (2007). Rapid regulation of Na^+ fluxes and ammonia excretion in response to acute environmental hypoxia in the Amazonian oscar, *Astronotus ocellatus*. *American Journal of Physiology. Regulatory, Integrative and Comparative Physiology*, *292*(5), R2048–R2058. https://doi.org/10.1152/ajpregu.00640.2006

Wood, C. M., & Randall, D. J. (1973a). The influence of swimming activity on water balance in the rainbow trout (*Salmo gairdneri*). *Journal of Comparative Physiology. A, Sensory, Neural, and Behavioral Physiology*, *82*(3), 257–276.

Wood, C. M., & Randall, D. J. (1973b). Sodium balance in the rainbow trout (*Salmo gairdneri*) during extended exercise. *Journal of Comparative Physiology, B: Biochemical, Systems, and Environmental Physiology*, *82*(3), 235–256.

Wood, C. M., Ruhr, I. M., Schauer, K. L., Wang, Y., Mager, E. M., McDonald, M. D., … Grosell, M. (2019). The osmorespiratory compromise in the euryhaline killifish: Water regulation during hypoxia. *Journal of Experimental Biology*, *222*, jeb204818. https://doi.org/10.1242/jeb.204818

Yamamoto, N., Yoneda, K., Asai, K., Sobue, K., Tada, T., Fujita, Y., … Kato, T. (2001). Alterations in the expression of the AQP family in cultured rat astrocytes during hypoxia and reoxygenation. *Brain Research. Molecular Brain Research*, *90*(1), 26–38. https://doi.org/10.1016/s0169-328x(01)00064-x

Zhao, S., & Fernald, R. D. (2005). Comprehensive algorithm for quantitative real-time polymerase chain reaction. *Journal of Computational Biology*, *12*(8), 1047–1064. https://doi.org/10.1089/cmb.2005.12.1047

SUPPORTING INFORMATION

Additional supporting information may be found online in the Supporting Information section.

How to cite this article: Ruhr IM, Wood CM, Schauer KL, et al. Is aquaporin-3 involved in water-permeability changes in the killifish during hypoxia and normoxic recovery, in freshwater or seawater? *J Exp Zool*. 2020;1–15. https://doi.org/10.1002/jez.2393